Oxidations of ER$_3$ (E = P, As, or Sb) by Hydrogen Peroxide: Methylrhenium Trioxide as Catalyst

Mahdi M. Abu-Omar and James H. Espenson*

Contribution from the Ames Laboratory and Department of Chemistry, Iowa State University, Ames, Iowa 50011

Received June 17, 1994[⊗]

Abstract: Catalytic and noncatalytic conversions of tertiary phosphines to their oxides by hydrogen peroxide have been investigated. The catalyst is methylrhenium trioxide, CH_3ReO_3. The kinetics were investigated in acetonitrile—water (1:1 by volume) at 25 °C. Stepwise interactions between CH_3ReO_3 and H_2O_2 form $CH_3Re(\eta^2-O_2)(O)_2(OH_2)$, **A**, and $CH_3Re(\eta^2-O_2)_2(O)(OH_2)$, **B**. In CH_3CN-H_2O (1:1 v/v) the equilibrium constants are $K_1 = 13 \pm 2$ L mol^{-1} and $K_2 = 136 \pm 28$ L mol^{-1} at pH 1.0 and 25 °C. The forward and reverse rate constants for the formation of **A** in this medium are $k_1 = 32.5 \pm 0.3$ L mol^{-1} s^{-1} and $k_{-1} = 3.0 \pm 0.2$ s^{-1}. Systematic changes in the substituents on phosphorus were made to vary the nucleophilicity of the phosphine and its cone angles; the kinetic effects are discernible, although they lie in a narrow range. Triphenylarsine and triphenylstibine were also studied, and their rates are within a factor of 2 of that for PPh$_3$. The rhenium peroxides **A** and **B** show a small difference in reactivity. The bimolecular reactions between **A** and most of the phosphines have rate constants of the order 10^5 L mol^{-1} s^{-1}. The kinetic data support a mechanism that allows nucleophilic attack of the substrate at the rhenium peroxides.

Introduction

More severe environmental constraints and regulations necessitate the reduction of waste byproducts in chemical processes. Most widely used oxidants, such as permanganate and dichromate salts, suffer from high costs for waste and byproduct cleanup.[1] Hydrogen peroxide is an appealing substitute since its only reduction product is water, eq 1.

$$H_2O_2 \rightarrow H_2O + \{O\} \qquad (1)$$
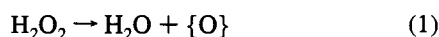
Because hydrogen peroxide reactions are often very slow, a catalyst is needed in most instances to activate H_2O_2. Such a catalyst must be able to transfer a single oxygen atom to a substrate and to accelerate the reaction to bypass the free-radical side reactions of peroxide. An organometallic oxide, CH_3ReO_3, was reported to be an excellent catalyst for olefin epoxidation by hydrogen peroxide.[2] The $CH_3ReO_3-H_2O_2$ system generates a potent oxidant far more kinetically competent than H_2O_2 itself. This catalyst offers these advantages: it is soluble and stable in many solvents including water, stable toward high concentrations of acid (pH 0—3), stable in air, easily purified by sublimation and recrystallization, and employable either homogeneously or (after immobilization) heterogeneously.

We have recently reported[3] the catalytic conversion of the thiolatocobalt complex $(en)_2CoSCH_2CH_2NH_2^{2+}$ (here CoSR^{2+}) by $CH_3ReO_3-H_2O_2$ to the sulfenato complex (CoS(O)R^{2+}) and then much more slowly to the sulfinato complex (CoS(O)$_2$R^{2+}) by a mechanism in which the coordinated sulfur nucleophilically attacks the 1:1 η^2-peroxo—rhenium compound. The catalytic oxidation of bromide ions was studied by following the formation of bromine and the concurrent catalytic disproportionation of hydrogen peroxide.[4] The mechanism proposed for

bromine formation involved a nucleophilic attack of Br$^-$ on a peroxide oxygen, the result of which is oxygen transfer to substrate:
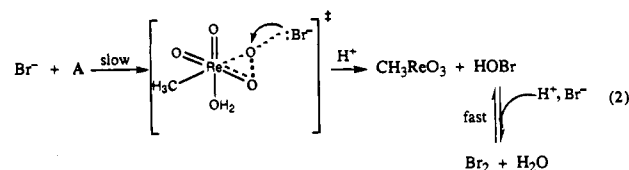
The investigation of the rhenium catalyst has now been extended to organic phosphines, Ar$_3$P mostly, and to triphenylarsine and triphenylstibine. We have determined the different reactivities of these substrates toward the catalytically active 1:1 adduct in the $CH_3ReO_3-H_2O_2$ system, and in two instances toward the 2:1 adduct as well. Systematic changes of the nucleophilicity and the cone angles of phosphorus were made.

The peroxide oxidation of PR$_3$ is catalyzed by Mo(VI), an electrophilic, high-oxidation-state complex (eqs 3 and 4).[5,6] It remains to be seen whether the mechanisms are similar.
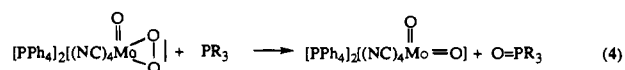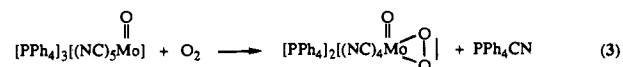
Experimental Section

Materials. The solvent was a mixture of acetonitrile and water (1:1 v/v). HPLC grade acetonitrile (Fisher) was used, and high-purity water was obtained by passing laboratory distilled water through a Millipore-Q water purification system. Hydrogen peroxide solutions prepared by diluting 30% H_2O_2 were standardized daily by iodometric titration. Triphenylphosphine was recrystallized from diethyl ether. The other phosphines were purchased commercially. 1,3,5-Triaza-7-phosphaada-

[⊗] Abstract published in *Advance ACS Abstracts*, December 1, 1994.

(1) Strukul, G. In *Catalytic Oxidations with Hydrogen Peroxide as Oxidant*; G. Strukul, Ed.; Kluwer Academic Publishers: Dordrecht, 1992.

(2) Herrmann, W. A.; Fischer, R. W.; Marz, D. W. *Angew. Chem., Int. Ed. Engl.* **1991**, *30*, 1638.

(3) Huston, P.; Espenson, J. H.; Bakac, A. *Inorg. Chem.* **1993**, *32*, 4517.

(4) Espenson, J. H.; Pestovsky, O.; Huston, P.; Staudt, S. *J. Am. Chem. Soc.* **1994**, *116*, 2869.

(5) Arzoumanian, H.; Pétrignani, J. F.; Pierrot, M.; Ridouane, F.; Sanchez, J. *Inorg. Chem.* **1988**, *27*, 3377.

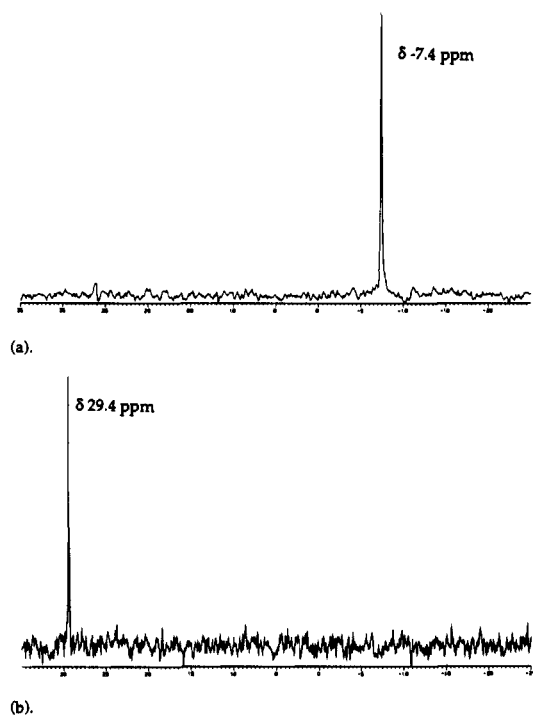(6) Mimoun, H. *J. Mol. Catal.* **1980**, *7*, 1.

Methylrhenium Trioxide Catalyzed Oxidation

J. Am. Chem. Soc., Vol. 117, No. 1, 1995 273

(a).

(b).

Figure 1. $^{31}P\{^1H\}$ NMR spectra of $(p\text{-}ClC_6H_4)_3P$ (a) with a catalytic amount of CH_3ReO_3 and (b) after addition of H_2O_2 to give $(p\text{-}ClC_6H_4)_3P=O$.
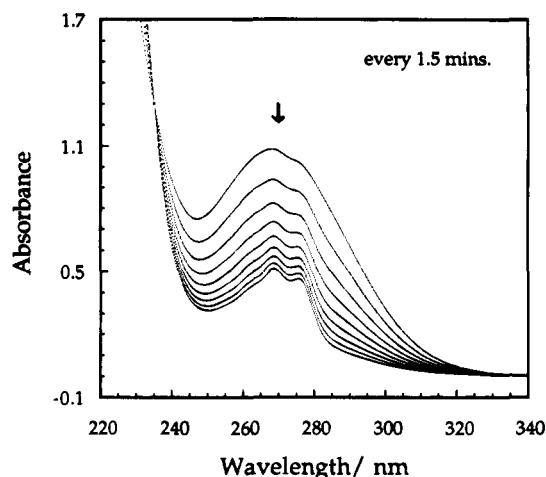
mantane (PTA), a gift from D. J. Darensbourg, was recrystallized from ethanol.[7] The purity of the starting reagents was checked by ^1H and ^{31}P NMR.

Methylrhenium trioxide[8] was purified by vacuum sublimation, followed by recrystallization from CH_2Cl_2—hexane and a final sublimation. The purity of the final product was checked in CH_2Cl_2 solution spectroscopically. IR: 1000 (w), 967 cm^{-1} (vs).[9] ^1H NMR: δ 2.63 ppm in $CDCl_3$.[10] UV—vis in H_2O: 239 nm (ϵ 1900 L mol^{-1} cm^{-1}), 270 nm (ϵ 1300 L mol^{-1} cm^{-1}).[11] Stock solutions of CH_3ReO_3 were prepared in water, protected from light, stored at -5 °C, and used within 10 days. The concentration was determined spectrophotometrically each day.

^1H NMR spectra were obtained with a Nicolet 300 MHz spectrometer, referenced to Me_4Si. $^{31}P\{^1H\}$ NMR spectra were recorded on a Varian VXR-300 spectrometer, with neat H_3PO_4 as the external reference.

Product Analysis. The phosphine oxides were characterized by ^1H and ^{31}P NMR. Figure 1 shows representative $^{31}P\{^1H\}$ spectra of tris-(p-chlorophenyl)phosphine and the oxide it produced. The near-UV spectra of the products showed the vibronic structure characteristic of phosphine oxides.[12] In addition to the ^{31}P NMR identification, 1,3,5-triaza-7-phosphaadamantane oxide was characterized by mass spectrometry: EI m/z, 173 (M); CI m/z, 174 (M + 1), 191 (M + 1 + NH_3).

Kinetic Studies. The kinetic studies were performed at 25.0 ± 0.2 °C in 1:1 (v/v) CH_3CN—H_2O, containing 0.10 M perchloric acid unless specified otherwise. The acid was present since it greatly stabilizes the CH_3ReO_3—H_2O_2 mixture against decomposition in aqueous and semiaqueous solutions. The air-sensitive substrates, methyldiphe-

(7) Diagle, D. J.; Peppermann, A. B., Jr.; Vail, S. L. *J. Heterocycl. Chem.* **1974**, *17*, 407.

(8) Herrmann, W. A.; Kuhn, F. E.; Fischer, R. W.; Thiel, W. R.; Ramao, C. C. *Inorg. Chem.* **1992**, *31*, 4431.

(9) Herrmann, W. A.; Kiprof, P.; Rydpal, K.; Tremmel, J.; Blom, R.; Alberto, R.; Behm, J.; Albach, R. W.; Bock, H.; Solouki, B.; Mink, J.; Lichtenberger, D.; Gruhn, N. E. *J. Am. Chem. Soc.* **1991**, *113*, 6527.

(10) Beattie, I. R.; Jones, P. J. *Inorg. Chem.* **1979**, *18*, 2318.

(11) Kunkely, H.; Turk, T.; Teixeira, C.; deMeric de Bellefon, C.; Herrmann, W. A.; Volger, A. *Organometallics* **1991**, *10*, 2090.

(12) (a) Jaffé, H. H. *J. Chem. Phys.* **1954**, *22*, 1430. (b) Hudson, R. F. *Structure and Mechanism in Organophosphorus Chemistry*; Academic Press: New York, 1965.

Figure 2. Repetitive spectral changes at 1.5-min intervals for the oxidation of 1.0×10^{-4} M $(p\text{-}CF_3C_6H_4)_3P$ with 3.0×10^{-3} M H_2O_2 in the presence of 2.0×10^{-6} M CH_3ReO_3 at pH 1.0 in 1:1 CH_3CN—H_2O.
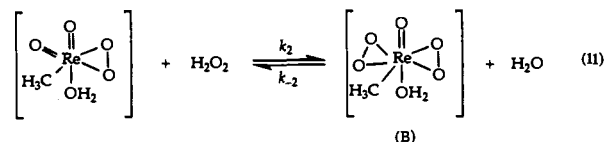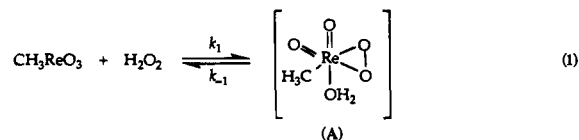
nylphosphine, tri-p-tolylphosphine, and tri-o-tolylphosphine, were studied under argon. Substrates that are not air-sensitive behaved the same whether protected by argon or not. Quartz cuvettes with different optical path lengths (0.1—10 cm) were used. The temperature was maintained by a thermostated water-filled cuvette holder. The reaction mixtures were incubated in the holder for at least 10 min to allow for temperature equilibration.

For kinetic studies by spectrophotometry, conventional (Shimadzu UV-2101PC) and stopped-flow (Sequential DX-17MV, Applied Photophysics Ltd.) instruments were used. The absorbance loss of the phosphine in the near-UV region (250—285 nm) was recorded. The product also absorbs in this region, but <0.2 times as strongly.[12] For example, the molar absorptivity of triphenylphosphine at 265 nm is 1.10×10^4 L mol^{-1} cm^{-1} and that of triphenylphosphine oxide at 265 nm is 2.0×10^3 L mol^{-1} cm^{-1}.[12] Typical repetitive spectral scans for the reaction of tris(p-(trifluoromethyl)phenyl)phosphine are displayed in Figure 2.

In many circumstances the most useful kinetic data were from the initial stage of the reaction, although the reactions were usually followed over the full time course. The initial reaction rates were calculated from the initial 5—7% of reaction. Under other conditions, however, the reactions followed first-order kinetics. The pseudo-first-order rate constant was evaluated by nonlinear fitting of the absorbance—time curves to a single-exponential decay equation, with $k_\psi = k_1[\text{Re}]_T$:

$$Abs_t = Abs_\infty + (Abs_0 - Abs_\infty)e^{-k_\psi t} \qquad (5)$$

Equilibrium Studies. The adoption of 1:1 CH_3CN—H_2O as solvent required the remeasurement of the equilibrium constants for the formation of **A** and **B**, eq I and II. They were determined from the

(A)

(B)

absorbances in the range 360—420 nm over a wide range of hydrogen peroxide concentrations. The data were fitted to eq 6.[13]

(13) Yamazaki, S.; Espenson, J. H.; Huston, P. L. *Inorg. Chem.* **1993**, *32*, 4368.

$$\frac{(\text{absorbance})_\lambda}{[\text{Re}]_T} = \frac{\epsilon_A K_1[H_2O_2] + \epsilon_B K_1 K_2[H_2O_2]^2}{1 + K_1[H_2O_2] + K_1 K_2[H_2O_2]^2} \quad (6)$$

Results

Equilibrium Constants. Compounds **A** and **B** are the monoperoxo and diperoxo derivatives of hydrogen peroxide and CH_3ReO_3.[13] The tight binding of water to the rhenium atom of **B** was shown in solution (by ^{17}O NMR) and in its diglyme adduct in the solid state (by X-ray diffraction).[14] Plausibly, **A** also has a coordinated water molecule; it is shown as such in eq I, but its presence has not been verified. Proton transfer from the entering hydrogen peroxide to an oxo ligand has been suggested as the mechanism for the formation of **A**.[15]

The new spectrophotometric determinations of K_1 and K_2 were carried out in 1:1 v/v CH_3CN-H_2O at 25.0 °C; the solutions contained 0.10 M perchloric acid, 1.00 mM CH_3ReO_3, and 0.0010–0.70 M H_2O_2. The spectra were recorded at wavelengths of 360, 380, 400, and 420 nm. A typical fit to eq 6 of the data at one of the wavelengths is shown in Figure 3. Absorbance data collected at the four different wavelengths were then fitted globally to eq 5 with the program GraFit. The equilibrium constants are $K_1 = 13 \pm 2$ L mol^{-1} and $K_2 = 136 \pm 28$ L mol^{-1}. The values obtained here are not much different from those reported at $\mu = 0.10$ M in aqueous solution, $K_1 = 7.7$ L mol^{-1} and $K_2 = 145$ L mol^{-1}.[13]

Oxygen Transfer from CH_3ReO_3. We investigated the possibility of transfer of an oxygen atom from CH_3ReO_3 to PPh_3 under the conditions used in this study. This reaction had been reported elsewhere,[16] albeit under different conditions. With $[PPh_3]$ and $[CH_3ReO_3]$ on the order of 10^{-4} M, the peroxide-free reaction took approximately 4 days, Figure 4. In comparison, the catalytic reactions of PPh_3 with the $H_2O_2-CH_3ReO_3$ system under these conditions take 5 min or less to reach completion. Since the oxo-transfer reaction from CH_3ReO_3 to PPh_3 is much slower than the reaction of PPh_3 with the $H_2O_2-CH_3ReO_3$ catalytic system, reaction III could be neglected.

$$CH_3ReO_3 + PPh_3 \xrightarrow{k_t} [CH_3Re^V O_2] + O{=}PPh_3 \quad (III)$$

The Uncatalyzed Oxidations. Reactions in the absence of CH_3ReO_3 were examined with $[H_2O_2] \geq 10[ER_3]$, the same conditions used for the catalyzed reactions. The disappearance of the substrate was followed in the near-UV region, 260–285 nm. The uncatalyzed oxidations followed first-order kinetics in both phosphine and hydrogen peroxide, eq 7. The second-order rate constants for the uncatalyzed reactions, k_u, are reported in Table 1.

$$\left(\frac{d[ER_3]}{dt}\right)_u = k_u[H_2O_2][ER_3] \quad (7)$$

Catalysis with CH_3ReO_3: An Overview. Typical repetitive-scan spectra for the catalytic oxidation of tris(p-(trifluoromethyl)phenyl)phosphine are shown in Figure 2. The overlaid spectra feature an isosbestic point at 235 nm, indicating that no intermediates attain an appreciable concentration. Addition of small amounts ($\leq 10^{-5}$ M) of CH_3ReO_3 dramatically changed the shape of the kinetic traces. The reactions with rhenium were much faster and appeared to follow zeroth-order kinetics during

(14) Herrmann, W. A.; Fischer, R. W.; Schere, W.; Rauch, M. H. *Angew. Chem., Int. Ed. Engl.* **1993**, *32*, 1157.

(15) Pestovsky, O.; van Eldik, R.; Huston, P.; Espenson, J. H. Submitted for publication.

(16) Felixberger, J. K.; Kuchler, J. G.; Herdtweck, E.; Paciello, R. A.; Herrmann, W. A. *Angew. Chem., Int. Ed. Engl.* **1988**, *27*, 946.
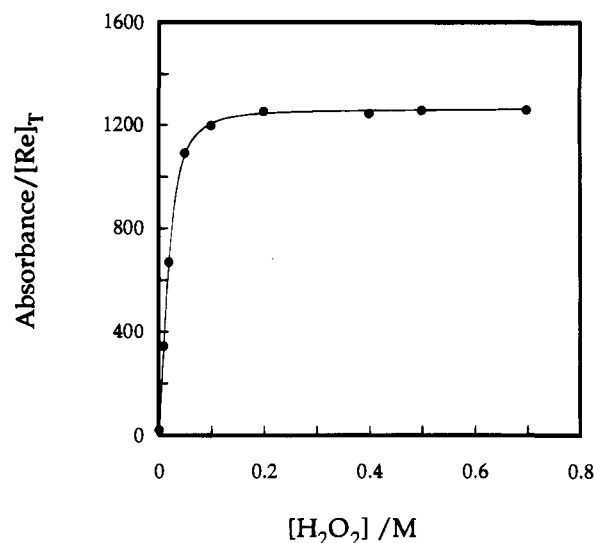

Figure 3. Plot of the absorbance at 360 nm of $CH_3ReO_3-H_2O_2$ solutions as a function of $[H_2O_2]$ at $[Re]_T = 1.0$ mM. The fit to eq 6 yields $K_1 = 14 \pm 2$ M^{-1} and $K_2 = 128 \pm 22$ M^{-1}. Conditions: pH 1.0 in 1:1 CH_3CN-H_2O at 25.0 °C.
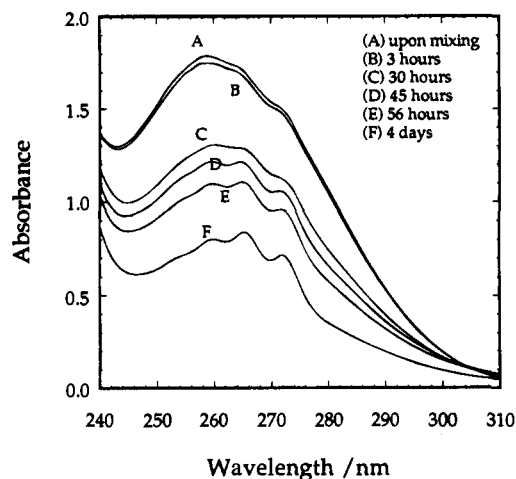
Figure 4. Changes in the UV spectrum of 1.8×10^{-4} M PPh_3 and 1.0×10^{-4} M CH_3ReO_3 over a period of 4 days in 1:1 CH_3CN-H_2O at pH 1.0.

the initial part of the reaction, but an approximate single exponential toward the end. This is illustrated in Figure 5 for a tris(pentafluorophenyl)phosphine. At high substrate concentrations, a zeroth-order limit in substrate was reached (see eq 8); this is demonstrated in the inset of Figure 5 for PPh_3. The rate of the catalyzed reaction showed first-order dependences on $[H_2O_2]$ and $[Re]_T$.

When $[\mathbf{B}]$ was negligible (*i.e.*, eq II was unimportant), which was realized at low $[H_2O_2]$,[13] the reactive form of the catalyst was **A** (the 1:1 adduct); hence, the simplified catalytic scheme is described by eqs I and IV.
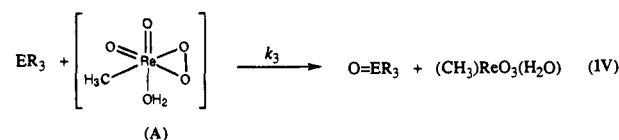

The rate equation derived from these two reactions by means of the steady-state approximation for $[\mathbf{A}]$ is given by eq 8, in which $[\text{Re}]_T = [CH_3ReO_3] + [\mathbf{A}]$. The rate equation here applies to conditions where $[\mathbf{B}]$ is negligible, and therefore,

Table 1. Summary of Rate Constants for Reactions of **A** and **B**[a]

substrate	k_u (L mol⁻¹ s⁻¹) uncatalyzed	k_3 (L mol⁻¹ s⁻¹) catalyst A	k_4 (L mol⁻¹ s⁻¹) catalyst B	activation = k_3/k_u
P(p-CH$_3$C$_6$H$_4$)$_3$	4.1 ± 0.4	(9.4 ± 0.6) × 10^5		2.3 × 10^5
P(C$_6$H$_5$)$_3$	3.0 ± 0.1	(7.3 ± 0.5) × 10^5	(2.16 ± 0.05) × 10^6	2.4 × 10^5
P(p-ClC$_6$H$_4$)$_3$	1.87 ± 0.06	(4.8 ± 0.2) × 10^5		2.6 × 10^5
P(p-CF$_3$C$_6$H$_4$)$_3$	0.71 ± 0.04	(3.4 ± 0.2) × 10^5		4.8 × 10^5
P(o-CH$_3$C$_6$H$_4$)$_3$	0.119 ± 0.002	(1.90 ± 0.06) × 10^5		1.6 × 10^6
P(C$_6$H$_5$)$_2$(CH$_3$)[b]	7.5 ± 0.6	(39 ± 4) × 10^5		5.2 × 10^5
PTA		(3.2 ± 0.2) × 10^3		
P(C$_6$F$_5$)$_3$	0.0016 ± 0.0001	130 ± 4	347 ± 25	8 × 10^4
As(C$_6$H$_5$)$_3$	0.084 ± 0.001	(3.7 ± 0.3) × 10^5		4.4 × 10^6
Sb(C$_6$H$_5$)$_3$	1.33 ± 0.04	(5.3 ± 0.4) × 10^5		4 × 10^5

[a] In 1:1 CH$_3$CN−H$_2$O at 0.10 M HClO$_4$ and 25.0 °C. [b] 1.0 × 10⁻⁴ M HClO$_4$.
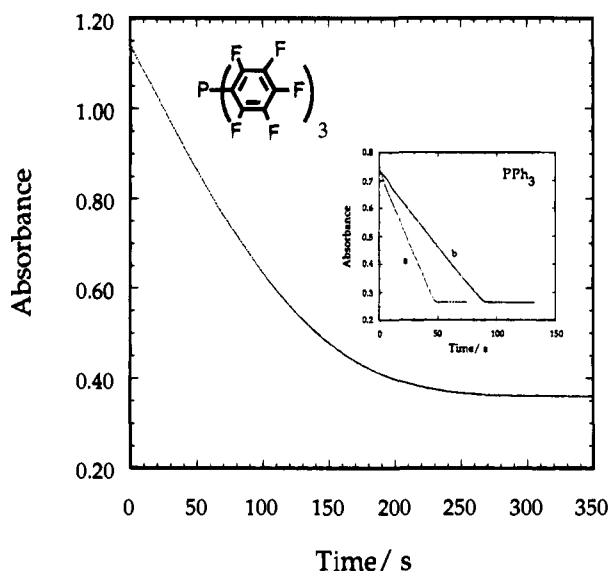
Figure 5. A typical kinetic trace for a catalytic phosphine oxidation monitored spectrophotometrically at 260 nm. Conditions: 25.0 °C, 0.10 M HClO$_4$, 5.0 × 10⁻⁵ M CH$_3$ReO$_3$, 0.03 M H$_2$O$_2$, and 8.0 × 10⁻⁵ M P(C$_6$F$_5$)$_3$. Inset: Kinetic data in the form of absorbance (λ = 270 nm)−time curves for two experiments with [PPh$_3$]$_0$ = [Re]$_T$ = 8.0 × 10⁻⁵ M at (a) [H$_2$O$_2$] = 2.5 × 10⁻⁴ M and (b) 5.0 × 10⁻⁴ M.

Figure 6. The plot of the pseudo-first-order rate constants, corrected for the contribution of the uncatalyzed reaction, for the oxidation of PPh$_3$ (0.5 × 10⁻³ M) by H$_2$O$_2$ (5.0 × 10⁻⁵ M) at 25.0 °C and pH 1.0 in 1:1 CH$_3$CN−H$_2$O. The linear variation of k_ψ with the catalyst concentration affords k_1 = 32.5 ± 0.3 L mol⁻¹ s⁻¹.

oxidation of the ER$_3$ by **B** is unimportant (unless, of course, the trace of **B** was exceptionally reactive compared to a larger amount of **A**, a possibility that will be ruled out subsequently).
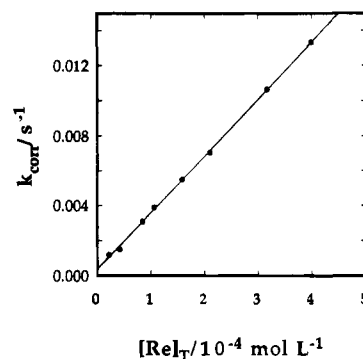
$$v_c = \left(\frac{d[ER_3]}{dt}\right)_c = \frac{k_1 k_3 [Re]_T [H_2O_2][ER_3]}{k_{-1} + k_3[ER_3] + k_1[H_2O_2]} \quad (8)$$

Kinetics at High [PPh$_3$]. Inspection of eq 8 reveals that, at high concentrations of PPh$_3$, such that k_3[PPh$_3$] ≫ k_{-1}, the limiting form of the rate law is
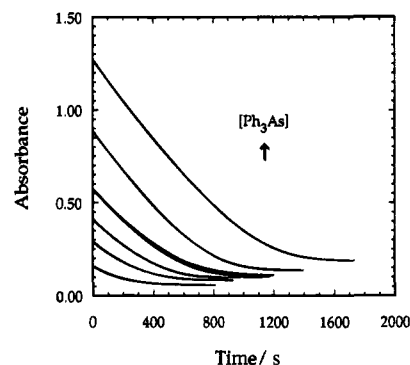
$$v_c = \left(\frac{d[PPh_3]}{dt}\right)_c = k_1 [Re]_T [H_2O_2] \quad (9)$$

An extensive set of experiments were carried out with limiting [H$_2$O$_2$] (5.0 × 10⁻⁵ M) and high [PPh$_3$] (0.5 × 10⁻³ M), and over a wide range of [Re]$_T$ (0.22−4.0 × 10⁻⁴ M). The kinetic traces under these conditions were fitted by a single exponential, eq 5, indicating that eq 9 was then valid.

In a series of such experiments, changes in the initial concentrations of H$_2$O$_2$ and PPh$_3$ had no effect on the apparent first-order rate constants. As eq 9 suggests, the values of k_ψ were directly proportional to [Re]$_T$. A plot of the values of the experimental rate constants corrected for the uncatalyzed contribution versus [Re]$_T$ is given in Figure 6. The slope of

Figure 7. A family of kinetic traces for the oxidation of triphenylarsine, monitored spectrophotometrically at 250 nm. Conditions: 25.0 °C, pH 1.0, 3.5 × 10⁻⁶ M CH$_3$ReO$_3$, 4.9 × 10⁻⁴ M H$_2$O$_2$,with [Ph$_3$As]/10⁻⁵ M = 0.5, 1.0, 1.5, 2.1, 2.5, 3.5, and 5.0.

this line gives the value of k_1 = 32.5 ± 0.3 L mol⁻¹ s⁻¹ at 25.0 °C in 1:1 CH$_3$CN−H$_2$O at 0.10 M HClO$_4$.

Kinetics at Variable [ER$_3$]: Initial-Rate Method. As can be seen from eq 8, the conditions needed for evaluation of k_3 and k_{-1} are low [H$_2$O$_2$], with [ER$_3$] varied in the region where k_{-1} and k_3[ER$_3$] are comparable. These conditions were achieved in a series of experiments using the substrates Ph$_3$P and Ph$_3$As. The concentrations for the first series were 3.0 × 10⁻⁴ M H$_2$O$_2$, 4.0 × 10⁻⁵ M CH$_3$ReO$_3$, and (1−15) × 10⁻⁵ M PPh$_3$. The second series was performed with 4.9 × 10⁻⁴ M H$_2$O$_2$, 3.5 × 10⁻⁶ M CH$_3$ReO$_3$, and (0.50−10) × 10⁻⁵ M Ph$_3$-As. Representative traces are shown for [Ph$_3$As] variation in Figure 7. The shapes of the absorbance−time recordings, as mentioned previously, are typical of Michaelis−Menten kinetics, being zeroth-order during the initial part of the reaction and approaching first-order toward the end.

276   *J. Am. Chem. Soc., Vol. 117, No. 1, 1995*

Abu-Omar and Espenson

Figure 8. Variations of the initial rate of reaction, corrected for the contribution of the uncatalyzed reaction, with (a) [PPh3] and (b) [Ph3-As]. The curves show the fit of these data to the rate law (eq 8) applicable when [**B**] is negligible. Conditions: 25.0 °C, pH 1.0, (a) 4.0×10^{-5} M CH_3ReO_3, 3.0×10^{-4} M H_2O_2; (b) 3.5×10^{-6} M CH_3-ReO_3, 4.9×10^{-4} M H_2O_2.

The initial-rate method was applied in each case and gave a value of v_i that was then corrected for the contribution of the uncatalyzed reaction. In every case the correction amounted to no more than 10% of the total rate ($v_{Tot} = v_u + v_c$). The plots of initial rate, so corrected, versus [PPh3] and [AsPh3] are shown in Figure 8. In the limit of high [PPh3] or [Ph3As], the initial rate reached a plateau to give the already-determined value of k_1; in this limit, recall that the rate law is reduced to the form shown in eq 9. Visual inspection of the plots in Figure 8 confirms this.

The value for k_{-1} was obtained from the fit to eq 8. In this calculation, k_1 was fixed at 32.5 L mol^{-1} s^{-1}, as given above, and (from the next section) $k_3(\text{PPh}_3) = 7.3 \times 10^5$ L mol^{-1} s^{-1} and $k_3(\text{Ph}_3\text{As}) = 3.7 \times 10^5$ L mol^{-1} s^{-1}. This led[17] to $k_{-1} = 3.0 \pm 0.2$ s^{-1} at 25.0 °C in CH_3CN-H_2O at pH 1.0. The value of k_{-1} from these kinetic investigations is consistent with that calculated independently from the equilibrium study, with $k_{-1} = k_1/K_1 = 2.5 \pm 0.3$ s^{-1}.

Catalysis with CH3ReO3: Determination of k_3 for All Substrates. Two types of initial-rate studies were performed to determine the values for k_3. Both were carried out at low [H_2O_2], so the amount of **B** present would be negligible. The order of mixing was also significant; in order that [**B**] be negligible, hydrogen peroxide was added last. This prior equilibration is necessary because the rate at which **A** reacts with a phosphine is higher than that at which it is converted to **B**, or at least comparable; without this as a part of the protocol, **B** would not carry much of the reaction, and the kinetic situation would be rather more complex. In one series of experiments, [Re]$_T$ was varied $0-20 \times 10^{-5}$ M in the presence of $0.5-1.0$

---

(17) The data sets employed to determine values for k_{-1} and k_3 were fit iteratively to determine the best values for these rate constants.

Figure 9. Variation of the initial rate of reaction, corrected for the uncatalyzed reaction, with (a) [H_2O_2], $k_3 = (5.3 \pm 0.4) \times 10^5$ L mol^{-1} s^{-1} and (b) [Re]$_T$, $k_3 = (5.2 \pm 0.3) \times 10^5$ L mol^{-1} s^{-1} for Ph_3Sb at 25.0 °C and pH 1.0. Conditions: (a) 1.5×10^{-5} M Ph_3Sb, 8.0×10^{-6} M CH_3ReO_3; (b) 1.5×10^{-5} M Ph_3Sb, 1.0×10^{-4} M H_2O_2.

$\times 10^{-5}$ M ER_3 and $\sim 1.0 \times 10^{-4}$ M H_2O_2. The relationship between the corrected initial rate, $v_i(\text{corr})$ (corrected for the uncatalyzed contribution, which amounts to no more than 10% of the total rate), and [Re]$_T$ is linear as expected from eq 8. The data were fitted to eq 8, fixing k_1 and k_{-1} at 32.5 L mol^{-1} s^{-1} and 3.0 s^{-1}, respectively. This yielded k_3 values for the different substrates used in this study. Figure 9b illustrates the linear relationship between v_i and [Re]$_T$ for Ph_3Sb.

In the second series of experiments, [H_2O_2] was varied in the range $(0.5-3.5) \times 10^{-4}$ M. A plot of the corrected v_i versus [H_2O_2] was linear at this low [H_2O_2], where the denominator term in eq 8 that contains [H_2O_2] is negligible. These data were fitted to eq 8 to yield values for k_3. The values of k_3 obtained from these two studies were consistent with each other; see, for example, the k_3 value for Ph_3Sb given in Figure 9.

A global fit of the initial rates from both studies to eq 8 yielded a single k_3 value for each substrate. These second-order rate constants for the catalyzed reactions are tabulated alongside those for the uncatalyzed reactions in Table 1. The activation power of methylrhenium trioxide, defined as k_3/k_u, is also presented in Table 1. It shows an acceleration of 10^5-10^6 when compared with H_2O_2 alone.

Catalysis with CH3ReO3: The Role of B. Since **B**, like **A**, contains η^2-peroxide ligands, it is reasonable to anticipate its ability to oxidize phosphines as illustrated in reaction V.

The catalytic activity and kinetics of **B** were studied for two different phosphines, PPh_3 and $P(C_6F_5)_3$. Pseudo-first-order conditions were satisfied by using [**B**] $\geq 10[PR_3]_0$ and [$H_2O_2]_0$

Methylrhenium Trioxide Catalyzed Oxidation

J. Am. Chem. Soc., Vol. 117, No. 1, 1995 277

[B]/10⁻⁴ mol L⁻¹

Figure 10. Plot of the pseudo-first-order rate constant for the oxidation of PPh₃ (4.0 × 10⁻⁶ M) by **B** showing linear variation of k_ψ with [**B**]. The curve is a fit to the rate law under these conditions (eq 10). Conditions: 25.0 °C, pH 1.0, 4.0 × 10⁻⁶ M PPh₃, 0.10 M H₂O₂.

≥ 100[Re]$_T$ with CH₃ReO₃ and H₂O₂ equilibrated prior to addition of substrate. These conditions were simulated with the program KINSIM,[18] which uses Runge−Kutta and Gear methods to generate concentration−time profiles for the reaction scheme, given the rate constants and starting concentrations. The simulations showed that, under the conditions stated above, the rate should be first-order with respect to [PAr₃], as was indeed observed.

The reactions under these conditions occur much more rapidly and so were studied with the stopped-flow technique. For triphenylphosphine, [Re]$_T$ was varied over the range (1.5−14.5) × 10⁻⁵ M, with [H₂O₂] = 0.10 M and [PPh₃] = 4.0 × 10⁻⁶ M. The solutions of CH₃ReO₃ and H₂O₂ were allowed to equilibrate for a few minutes before PPh₃ was added. Under these conditions k_ψ becomes

$$k_\psi = k_4[\mathbf{B}] + \frac{k_3[\mathbf{B}]}{K_2[\text{H}_2\text{O}_2]} \quad (10)$$

The concentrations of **B** were calculated from K_1 and K_2 from the equilibrium study, and k_3 was fixed at 7.3 × 10⁵ L mol⁻¹ s⁻¹, determined independently (see above). The plot of k_ψ versus [**B**] is linear, with k_4 as the slope, Figure 10. The fit to eq 10 provided k_4 = (2.16 ± 0.05) × 10⁶ L mol⁻¹ s⁻¹ in 1:1 CH₃CN−H₂O at pH 1.0. It turned out that k_4 is about 3 times larger than k_3 for PPh₃. Although **B** is more reactive toward PPh₃ than **A**, the difference in reactivity is not very substantial, with k_4 not even an order of magnitude larger than k_3.

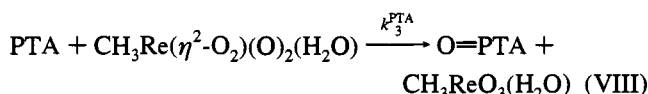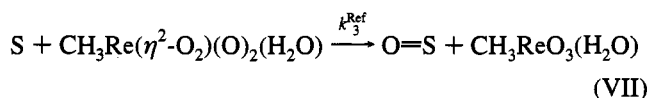For tris(pentafluorophenyl)phosphine, k_4 is 347 ± 27 L mol⁻¹ s⁻¹. Again, P(C₆F₅)₃ shows the same trend demonstrated by PPh₃, with $k_4 \sim 3k_3$.

The Case of PTA: Competition Kinetics. We chose to study this compound, 1,3,5-triaza-7-phosphaadamantane, because of the three electronegative nitrogen atoms; we sought to learn whether it is less reactive than PAr₃, as one might infer from the kinetic effects of varying the substituents on the aryl groups. Since PTA does not absorb in the UV region, the direct spectrophotometric method used with the other substrates could not be applied to its catalytic reaction with H₂O₂−CH₃ReO₃. Therefore, the reaction was investigated indirectly by utilizing competition reactions with a substrate that met two requirements: (1) it reacted with H₂O₂−CH₃ReO₃ at a rate comparable to that of PTA, and (2) it could be directly monitored spectrophotometrically. The rate constant for the reference substrate with **A** must be known independently.
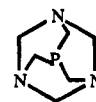
1,3,5-Triaza-7-phosphaadamantane (PTA)

The idea in such a competition reaction is to have both substrates, PTA and PAr₃ (where Ar = aromatic), for the catalytic active species **A** as illustrated by eqs VI−VIII. The concentrations must be adjusted so that the two rates are not too dissimilar.

$$\text{CH}_3\text{ReO}_3 + \text{H}_2\text{O}_2 \underset{k_{-1}}{\overset{k_1}{\rightleftharpoons}} \text{CH}_3\text{Re}(\eta^2\text{-O}_2)(\text{O})_2(\text{H}_2\text{O}) \quad (\text{VI})$$

$$\text{S} + \text{CH}_3\text{Re}(\eta^2\text{-O}_2)(\text{O})_2(\text{H}_2\text{O}) \overset{k_3^{\text{Ref}}}{\longrightarrow} \text{O=S} + \text{CH}_3\text{ReO}_3(\text{H}_2\text{O}) \quad (\text{VII})$$

$$\text{PTA} + \text{CH}_3\text{Re}(\eta^2\text{-O}_2)(\text{O})_2(\text{H}_2\text{O}) \overset{k_3^{\text{PTA}}}{\longrightarrow} \text{O=PTA} + \\ \text{CH}_3\text{ReO}_3(\text{H}_2\text{O}) \quad (\text{VIII})$$

The difference in initial rates for the reaction of S with H₂O₂−CH₃ReO₃ in the presence and absence of PTA gives the solution presented in eq 11, which is used in the competition reactions to evaluate k_3^{PTA}, the only unknown.

$$\frac{v^{\text{Ref}} - v}{v} = \frac{k_3^{\text{PTA}}[\text{PTA}]}{k_{-1} + k_3^{\text{Ref}}[\text{S}] + k_1[\text{H}_2\text{O}_2]} \quad (11)$$

Three different substrates were used independently to determine the rate constant for the reaction of PTA with **A**. Two of the substrates were aromatic phosphines, P(C₆F₅)₃ and P(p-CF₃C₆H₄)₃. In the case of P(C₆F₅)₃, 3.0 × 10⁻⁴ M CH₃ReO₃, 5 × 10⁻⁴ M of P(C₆F₅)₃, and 1.0 × 10⁻⁴ M H₂O₂ were used; [PTA] was varied from (0−1.5) × 10⁻³ M. The values of k_3-(P(C₆F₅)₃), k_{-1}, and k_1 were fixed at 130 L mol⁻¹ s⁻¹, 3.0 s⁻¹, and 32.5 L mol⁻¹ s⁻¹, respectively. The plot of [v^{Ref}(P(C₆F₅)₃) − v]/v, where V here and in eq 11 represents the initial rate of disappearance of the reference substrate, versus [PTA] is shown in Figure 11. The fit to eq 11 provided k_3^{PTA} = (3.24 ± 0.06) × 10³ L mol⁻¹ s⁻¹.

For the second substrate, (p-CF₃C₆H₄)₃P, the following concentrations were used: [(p-CF₃C₆H₄)₃P] = 8.0 × 10⁻⁶ M, [H₂O₂] = 0.6 × 10⁻³ M, [Re]$_T$ = 2.8 × 10⁻⁶ M, and [PTA] = (0−8.5) × 10⁻⁴ M. The fit to eq 11 gave k_3^{PTA} = (3.4 ± 0.2) × 10³ L mol⁻¹ s⁻¹.

p-Tolyl methyl sulfide, (p-CH₃C₆H₄)SCH₃, was also employed in this competition study, since its rate constant is closer to that for PTA. This thioether reacts cleanly with **A** to form the sulfoxide.[19] The rate constant k_3^{Ref} ((p-tolyl)SMe) is 4.3 × 10³ L mol⁻¹ s⁻¹.[19] The concentrations used in this investigation were [ArSMe] = 1.0 × 10⁻³ M, [H₂O₂] = 0.010 M, [CH₃-ReO₃] = 6.0 × 10⁻⁵ M, and [PTA] = (0−4.3) × 10⁻³ M. The fit to eq 11 gave k_3^{PTA} = (3.5 ± 0.2) × 10³ L mol⁻¹ s⁻¹. The k_3^{PTA} values from three independent studies agree within acceptable precision. In the competition experiments the concentrations of hydrogen peroxide used were low enough to avoid significant formation of **B**. Also, hydrogen peroxide was added to the reaction mixture last to assure that negligible amounts of **B** were present at the outset.

The Integrity of the Catalyst. Several tests were run to examine the stability of the catalyst under our reaction condi-

(18) Barshop, B. A.; Wrenn, C. F.; Frieden, C. *Anal. Biochem.* **1983**, *130*, 134.

(19) Vassell, K.; Espenson, J. H. Unpublished observations.
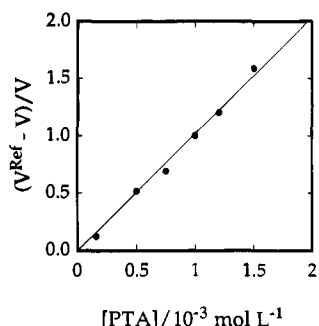
Figure 11. The rate-enhancement function, $[\nu_p(P(C_6F_5)_3) - \nu_s(PTA)]/$ $\nu_s(PTA)$, varies linearly with [PTA] according to eq 11 for competition experiments. Conditions: 25.0 °C, pH 1.0, 2.5 × 10⁻⁴ M P(C₆F₅)₃, 3.0 × 10⁻⁴ M CH₃ReO₃, 1.0 × 10⁻⁴ M H₂O₂.

Table 2. Substituent Effects on the Rate Constants for Substituted Phosphines[a]

phosphine	k_3 (L mol⁻¹ s⁻¹)	σ_p
P(p-CH₃C₆H₄)₃	(9.4 ± 0.6) × 10⁵	−0.17
P(C₆H₅)₃	(7.3 ± 0.5) × 10⁵	0.00
P(p-ClC₆H₄)₃	(4.8 ± 0.2) × 10⁵	0.23
P(p-CF₃C₆H₄)₃	(3.4 ± 0.2) × 10⁵	0.54

[a] In 1:1 CH₃CN−H₂O at 0.10 M HClO₄ and 25.0 °C.

tions. In one experiment that demonstrates the stability of the catalyst after many turnovers, [substrate] = 100[CH₃ReO₃] was employed. The concentrations used were as follows: 6.0 × 10⁻⁵ M Ph₃As, 6.0 × 10⁻⁷ M CH₃ReO₃, and 5.0 × 10⁻³ M H₂O₂. After the reaction was done, additional 4.0 × 10⁻⁵ M Ph₃As was added. The rate of catalytic oxidation was similar (93%) to that with the initial batch of Ph₃As, indicating stability and high percent of catalyst recovery. On a preparatory scale, 0.20 g (97% yield) of O=P(C₆F₅)₃ was isolated from the reaction of 0.20 g (3.8 × 10⁻⁴ mol) of P(C₆F₅)₃ with 1.0 × 10⁻³ mol of H₂O₂, employing 1.0 mg (4.0 × 10⁻⁶ mol, 1% of substrate) of catalyst, CH₃ReO₃. In a ¹H NMR experiment, conducted in CD₃CN as solvent, concentrations of Ph₃As and H₂O₂ that were >25 times that of CH₃ReO₃ were used. The intensity of the methyl-proton signal ($H_3C−ReO_3$) at 2.8 ppm indicated that all of the CH₃ReO₃ remained at the end of the reaction, within the limits of detection.

Discussion

It has been shown[13] that CH₃ReO₃ reversibly forms compounds **A** and **B** with H₂O₂ in aqueous solutions. We have also demonstrated that the same holds in 1:1 CH₃CN−H₂O. This points to a mechanism in which eqs I and II are involved in the catalytic cycle. In other words, the monoperoxo and diperoxo species from the interaction of CH₃ReO₃ and H₂O₂ could be anticipated to be the catalytically active species. Under conditions where [**B**] is negligible, at low peroxide concentrations, eq I is analogous to the formation of the Michaelis−Menten complex. The fact that the CH₃ReO₃ catalytic system follows Michaelis−Menten kinetics is of no surprise, since many catalytic systems tend to do so.

The experimentally-determined rate law in eq 8 has a denominator term containing [ER₃] as well as one containing [H₂O₂]. Therefore, this is a two-substrate system in its kinetics as well as in its chemistry. The key step in the catalytic cycle involves the reaction of one of the rhenium−peroxide complexes, **A** or **B**, with the substrate ER₃, as in eqs IV and V. This step is the stage at which the oxygen atom is excised by the substrate.

At low concentrations of peroxide, and in the presence of excess [ER₃], the reaction is first-order with respect to [H₂O₂].

This indicates that the active species under these conditions is adduct **A**, formed from the first equivalent of hydrogen peroxide. Were **B** the active species under these conditions, meaning that $k_4 \gg k_3$, even with [**B**] ≪ [**A**], second-order kinetics with respect to [H₂O₂] should have been observed. This can be seen by inspection of the full rate law. With the steady-state approximations for both peroxides, the full rate equation is given by

$$-\frac{d[ER_3]}{dt} =$$

$$\frac{k_1k_3[Re]_T[H_2O_2][ER_3] + \dfrac{k_1k_2k_4[Re]_T[ER_3][H_2O_2]^2}{k_4[ER_3] + k_{-2}}}{k_{-1} + k_3[ER_3] + k_1[H_2O_2] + \dfrac{k_1k_2[H_2O_2]^2}{k_4[ER_3] + k_{-2}}} \quad (12)$$

In the limit where [H₂O₂] is very small, the rate is given by

$$v = \left\{\frac{K_1k_2k_4[Re]_T[ER_3]}{k_{-2} + k_4[ER_3]}\right\}[H_2O_2]^2 \quad (13)$$

From this treatment the value of k_1 is 32.5 ± 0.3 L mol⁻¹ s⁻¹, which agrees with that obtained in the same medium using a different substrate, methyl tolyl sulfide.[19] The reverse rate constant for the formation of **A**, k_{-1} = 3.0 ± 0.2 s⁻¹, also agrees with an independent determination.[19]
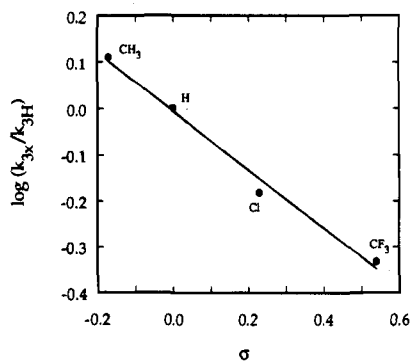
Also from eq 12, one can see that the limit of the rate at high [H₂O₂], where **B** comes into play, will be $v = k_4[Re]_T$ [ER₃]. To attain this, the prior equilibration of peroxide and CH₃ReO₃ as a part of the experimental protocol was necessary to simplify the kinetic treatment to this form. The experimental observation that the reaction followed pseudo-first-order kinetics at high [H₂O₂] was also confirmed to be consistent with the entire kinetic model by simulations with the program KINSIM.[18] The second-order rate constants, k_4, for the reaction of **B** with PPh₃ and P(C₆F₅)₃ differ by a factor of <3 from those for the reactions of **A**. This difference being less than an order of magnitude could be easily understood in light of the presence of two peroxo ligands in **B** rather than only one for **A**. Since the differences between the respective values of k_3 and k_4 for PPh₃ and P(C₆F₅)₃ are not very significant (only a factor of 3), the only conclusion that could be reached here is that both **A** and **B** have similar reactivities toward the phosphines.

The structure−reactivity correlations devised by Hammett[20,21] account for various reactions of *meta-* and *para-*substituted aromatic compounds. The values of σ, characteristic of substituent X in either a *meta* or *para* position, are available from the pK_a's of benzoic acids. Triarylphosphines from this study with different substituents on the *para* position were examined. Values for σ_p[22] are listed in Table 2 along with the k_3 values for the different phosphines. Figure 12 shows a plot of log(k_{3X}/k_{3H}) versus σ_p. The slope affords the reaction constant, $\varrho = -0.63$. The linear Hammett correlation suggested that all the phosphines react by the same mechanism in the CH₃-ReO₃−H₂O₂ catalytic system. The negative sign of the reaction constant is in agreement with nucleophilic attack of the phosphine on the electrophilic oxygen of the rhenium-bound peroxide. The fact that the reaction constant is near −1.0 suggests an early transition state with little P−O bond formation. One might also conclude, as suggested by a referee, that this

(20) Hammett, L. P. *Physical Organic Chemistry*; McGraw-Hill Book Co.: London, 1970.

(21) Hammett, L. P. *Chem. Rev.* **1935**, *17*, 125.

(22) Brown, H. C.; Okamota, Y. *J. Am. Chem. Soc.* **1958**, *80*, 4979.

Methylrhenium Trioxide Catalyzed Oxidation

*J. Am. Chem. Soc., Vol. 117, No. 1, 1995* 279

Figure 12. The Hammett correlation between the rate constants for the reactions of substituted phosphines with **A**. The linear fit yields the reaction constant ϱ of -0.63 ± 0.05.

value of the reaction constants shows that there is little change in charge density at phosphorus in the transition state.

The kinetic trend for the group 15 compounds (EPh$_3$) deserves comment. The rate constants for **A** follow the order P > Sb > As. It has been known for some time that aryl stibines are oxidized by alkaline hydrogen peroxide more readily (surprisingly) than aryl arsines.[23] Relative nucleophilic reactivity parameters (n_{Pt}) for a variety of nucleophiles were determined from the rates of their reactions toward the electrophile *trans*-[Pt(py)$_2$Cl$_2$].[24] The second-order rate constants for the reactions of Ph$_3$As and Ph$_3$Sb with *trans*-[Pt(py)$_2$Cl$_2$] are 2.3 and 1.8 L mol^{-1} s^{-1}, respectively. These rate constants are close, although in opposite order than those for **A**.

This still does not account for the small difference in the reactivities of Ph$_3$P and its arsine and stibine analogs. Such a resemblance in reactivities is not unprecedented. In fact some metal—peroxo catalysts have been used to oxidize arsines as well as phosphines (proving to be somewhat slower for arsines).[25] Some materials were found to be ineffective in catalyzing Ph$_3$P oxidation but very effective for catalytic oxidation of Ph$_3$As.[26] For example, Ru(η^2-O$_2$)(NO)(PPh$_3$)$_2$-(CO)(SCN)[27] oxidizes Ph$_3$As 3—4 times faster than Ph$_3$P under the same conditions. The relative rates of reaction of PhNEt$_2$, PhPEt$_2$, and PhAsEt$_2$ with EtI were found to be 1:500:70.[28] The difference here in reactivity between PhPEt$_2$ and PhAsEt$_2$ amounts to only a factor of 7. We thus conclude that the rhenium—peroxide catalyst **A** (and possibly **B** also) shows relatively little discrimination with respect to changing from phosphine to arsine or stibine. This might be a consequence of the high electrophilic activation of the η^2-coordinated peroxide ion (O$_2$)$^{2-}$ upon binding to Re(VII).

Hydrogen peroxide is generally thought to react with reducing nucleophiles by an S$_N$2 mechanism.[29] Since phosphines are nucleophilic in their chemistry,[12b] the mechanism of their oxidation by H$_2$O$_2$ is assumed to be nucleophilic attack by the phosphine on the O—O peroxide bond,[30] as depicted in eq IX.
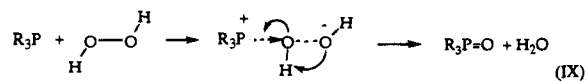
It is reasonable to assume that the same type of nucleophilic attack by ER$_3$ occurs in the CH$_3$ReO$_3$-catalyzed reaction. That is, the phosphorus, arsenic, or antimony atom attacks the oxygen of the coordinated peroxide ion of **A**.

Our proposed mechanism involves the formation of 1:1 and 2:1 peroxides **A** and **B** that then react with the substrate ER$_3$. The electron-poor rhenium makes the peroxide more electrophilic and, hence, more susceptible to nucleophilic attack, and a better source of an oxygen atom. The activation of hydrogen peroxide upon coordination to Re(VII) is remarkable, k_{cat}/k_{uncat} = (0.2—4.0) × 10^6. Such a large activation indicates major electronic changes in the peroxide upon coordination.

The possibility of coordination of the substrate prior to oxygen transfer should be considered at this stage. Such a mechanism would involve a four-membered-ring peroxo—metallacycle as shown in eq X. Mimoun proposed such a mechanism for reactive substrates, such as phosphines, sulfides, and amines with molybdenum peroxo complexes.[6] A different but closely related mechanism would be direct coordination as the first step, eq XI.
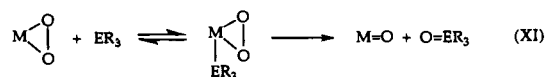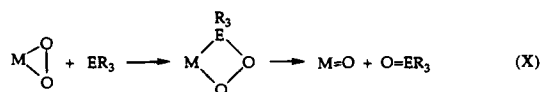
We sought evidence from the kinetic studies to support or reject such a mechanism as the major pathway for oxidation under the conditions of our investigations. But first let us consider some of the chemical and structural properties of the active peroxides **A** and **B**. From a structural point of view, **B**, the diperoxide, is seven-coordinate, with a coordinated water molecule that has been shown by ^{17}O NMR to be bound tightly in solution.[14] Then **B** is unlikely to coordinate a substrate molecule (ER$_3$) prior to oxygen transfer. Since **B** contains a tightly bound water molecule in its coordination sphere, it is not at all unreasonable to assume that **A** also contains a tightly bound water molecule, making the rhenium atom in **A** six-coordinate. Nevertheless, an argument (based on the ability of **B** to be seven-coordinate) in favor of substrate coordination prior to oxidation might still be made in the case of **A**. In so doing, however, one would be assigning different mechanisms to the pair of peroxides, which seems implausible.

Addition of excess OPPh$_3$ (5[ER$_3$]), which would compete with substrate for a coordination site on **A** were such involved, caused no retardation in the rate of oxidation. Another general tool for establishing substrate coordination in the catalytic oxidation process is the effect of steric hindrance on oxidation rates.[31] Whereas steric factors are known to be rather unimportant in typical electrophilic oxidations, such as the acid-catalyzed oxidation of sulfides with hydrogen peroxide,[32] they should play a major role in processes that involve the coordination of two reactants (catalyst and substrate here). For example, in the metal-catalyzed homogeneous hydrogenations of olefins where coordination of the olefin to the metal complex occurs, the retardation caused by the steric hindrance of the olefin is

(23) Sidgwick, N. V. *The Chemical Elements and their Compounds*; Oxford University Press: London, 1962; Vol. 1.

(24) Pearson, R. G.; Sobel, H.; Songstad, J. *J. Am. Chem. Soc.* **1968**, *90*, 319.

(25) (a) Cenini, S.; Fusi, A.; Capparella, G. L. *J. Inorg. Nucl. Chem.* **1971**, *33*, 3576. (b) Sutin, N.; Yandell, J. K. *J. Am. Chem. Soc.* **1973**, *95*, 4847.

(26) Chaloner, P. A. *Handbook of Coordination Catalysis in Organic Chemistry*; Butterworth & Co.: Boston, 1986.

(27) Graham, B. W.; Laing, K. R.; O'Connor, C. J.; Roper, W. R *J. Chem. Soc. Dalton Trans.* **1972**, 1237.

(28) Davies, W. C.; Lewis, W. P. *J. Chem. Soc.* **1934**, 1599.

(29) Hoffman, M.; Edwards, J. O. *Inorg. Chem.* **1977**, *16*, 3333 and references therein.

(30) Denney, D. B.; Goodyear, W. F.; Godstein, B. *J. Am. Chem. Soc.* **1960**, *82*, 1393.

(31) Bortolini, O.; Campello, E.; DiFuria, F.; Modena, G. *J. Mol. Catal.* **1982**, *14*, 63.

(32) Modena, G. *Gazz. Chim. Ital.* **1959**, *89*, 834.

remarkable;[33] the reactivity ratio of cyclohexene−1-methylcy-clohexene with certain Rh complexes is >40.[33]

Since (p-tolyl)$_3$P and (o-tolyl)$_3$P are electronically the same (Tolman's electronic parameter, ν,[34] for both is 2066.7 cm^{-1}) but sterically very different (cone angle, θ,[34] of 145° for the *para*-substituted methyl and 194° for the *ortho*-substituted methyl), we compared their reaction rates with **A**. The rate constants for the reactions of (p-tolyl)$_3$P and (o-tolyl)$_3$P with **A** (Table 1) are 9.4 × 10^5 and 1.9 × 10^5 L mol^{-1} s^{-1}, respectively. This small difference in rate, less than that observed in the uncatalyzed oxidations by H$_2$O$_2$, gives further support to the general validity of the "electrophilic" mechanism. That is, direct attack of the nucleophilic substrate on the electrophilic bound-peroxide oxygen is the major pathway accounting for the oxidations of ER$_3$. Therefore, we suggest the following structure for the transition state (a similar transition state could be drawn for **B** and ER$_3$):
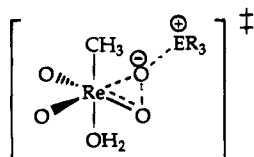
The oxidation of Ph$_3$P by many peroxo and oxo metal complexes is well-known.[35−38] Some of these results are compared with the work reported here in Table 3. The CH$_3$-ReO$_3$−H$_2$O$_2$ system is more reactive than most systems we are aware of that utilize O$_2$ in the formation of the (O$_2$)$^{2-}$ ion to bind in an η^2 fashion to the metal, such as Ru(η^2-O$_2$)(NO)-

(33) James, B. R. *Homogeneous Hydrogenation*, Wiley-Interscience: New York, 1973.

(34) Tolman, C. A. *Chem. Rev.* **1977**, 77, 313.

(35) Wang, W.-D.; Bakac, A.; Espenson, J. H. *Inorg. Chem.* **1993**, 32, 5034.

(36) Taqui Khan, M. M.; Chatterjee, D.; Siddiqui, M. R. H.; Bhatt, S. D; Bajaj, H. C.; Venkatasubramanian, K.; Moiz, M. A. *Polyhedron* **1993**, 12, 1443.

(37) Scott, S. L.; Bakac, A.; Espenson, J .H. *J. Am. Chem. Soc.* **1992**, 114, 4205.

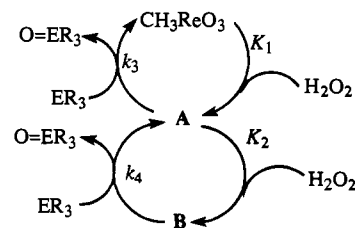(38) Durant, R.; Garner, C. D.; Hyde, M. R.; Mabbs, F. E. *J. Chem. Soc., Dalton Trans.* **1977**, 955.

Table 3. Summary of Rate Constants (25.0 °C) for the Oxidation of PPh$_3$

oxidant	rate constant/ L mol^{-1} s^{-1}	ref
H$_2$O$_2$	3.0 (2.94)	this work and ref 35
CH$_3$Re(η^2-O$_2$)(O)$_2$(H$_2$O)	7.3 × 10^5	this work
CH$_3$Re(η^2-O$_2$)$_2$(O)(H$_2$O)	2.1 × 10^6	this work
[Ru(EDTA)(H$_2$O)]$^-$/O$_2$	(1.4 × 10^{-4} s^{-1})	36
(H$_2$O)$_5$CrO^{2+}	2.1 × 10^3	37
(H$_2$O)$_5$CrOOH^{2+}	75	35
[MoO$_2$(S$_2$CNEt$_2$)$_2$]	1.1	38

(PPh$_3$)$_2$(CO)(SCN).[27] Also, as is evident from Table 3, CH$_3$-ReO$_3$−H$_2$O$_2$ adducts seem to be more effective than other metal complexes that activate H$_2$O$_2$, such as Cr−OOH^{2+}.

Conditions in this study were adjusted in order to obtain optimal kinetic parameters. We specially sought to make ν_{cat} ≫ ν_{uncat} so that the correction for the uncatalyzed reaction need not be made. Therefore, it was sometimes desirable to use CH$_3$-ReO$_3$ concentrations that were not much lower than substrate concentrations. However, the stability and catalytic ability of CH$_3$ReO$_3$ were tested by using substrate and H$_2$O$_2$ concentrations that were >100 times that of CH$_3$ReO$_3$. As well as we could tell, most of the CH$_3$ReO$_3$ remained at the end and was capable of performing many further catalytic cycles.

Conclusion. The following diagram presents the chemical transformations in diagrammatic form.